Materials Research. 2021; 24(4): e20200386
DOI: https://doi.org/10.1590/1980-5373-MR-2020-0386

Comparison Between Stainless Steels and Nickel Alloys Through Pitting Corrosion Resistance Electrochemical Tests

Ivy Frazão[a]*, *Rodrigo Magnabosco*[a], *Anna Delblanc*[b]

[a]*Centro Universitário FEI, Departamento de Engenharia de Materiais, Av. Humberto de Alencar Castelo Branco, 3972, 09850-901, São Bernardo do Campo, SP, Brasil*
[b]*Sandvik Materials Technology, Research & Innovation, 4371 SE-811 81 Sweden*

Received: August 25, 2020; Revised: March 08, 2021; Accepted: April 27, 2021

Critical pitting temperature (CPT) is one of the most accepted criteria for alloy classification concerning pitting corrosion. The techniques used nowadays to determine CPT have different parameters for alloys of different material classes, preventing the comparison between stainless steels and nickel based alloys. This study aims to compare the corrosion resistance of nickel based alloys and stainless steels with high corrosion resistance through potentiostatic tests for CPT determination, using a 3M $MgCl_2$ aqueous solution. CPT values were effectively determined for the stainless steels studied but the technique did not have the same efficiency for nickel based alloys due to the occurrence of crevice corrosion, even considering the higher PRE of nickel based alloys.

Keywords: CPT, pitting corrosion, high corrosion resistance alloys.

1. Introduction

CPT (critical pitting temperature) is widely used to analyze pitting corrosion resistance of stainless steel and other alloys, following ASTM G48[1] (using immersion tests) and ASTM G150[2] (for potentiostatic tests). It is also commonly used to compare the performance of materials on a given medium. Another way of analyzing pitting resistance is through the PRE-number, which can be calculated through PRE equation: PRE =% Cr + 3.3% Mo + 16% N. PRE based classifications are very common but it is not a safe way to analyze the pitting corrosion resistance, since it considers only the main chemical composition, regardless of the presence of intermetallic phases, precipitates, different surface finishing and other factors that influence pitting corrosion. High corrosion resistance alloys (CRA) with PRE higher than 47[3] tend to have CPT in 1M NaCl solutions above 95°C, which restrict the use of corrosion tests using the potentiostatic method proposed by ASTM G150, since corrosive sodium chloride solutions have boiling points close to 100°C. In addition, immersion corrosion methods such as the ones described in ASTM G48[1] have different tests methodologies for stainless steels or nickel alloys, therefore preventing a direct comparison of CPT results obtained from different materials using immersion tests.

Some polarization studies based on ASTM G150[2] alter the applied potential and chloride concentration aiming to have a more aggressive test environment, allowing CPT determination of high CRA[4-6]. These studies highlight that higher potentials and higher chloride concentrations promote a decrease on CPT values. Other studies[3,7] changed the electrolyte medium used in the potentiostatic test, with 3M $MgCl_2$ being one of the prominent electrolytes due to the high chloride concentration and higher boiling point (117°C)[8] in comparation with the conventional 1M NaCl solution used in ASTM G150[2] tests.

Another way to analyze corrosion resistance is by determining pitting potential (E_{pit}) through potentiodynamic polarization tests, which can be identified as a drastic increase in current density after the passive region on the polarization curve. This sudden increase in current may occur due to a disruption of the passive film induced by chlorides, characterizing the onset of pitting corrosion. However, the increase on current density may occur due to different mechanisms besides pitting corrosion, depending on the medium in which the material is located. For example, the potential for sudden current increase can occur due to the oxygen evolution potential, or due to transpassivation, which on this scenario is called as breakthrough potential (E_b)[9-12]. If pitting occurs at potentials higher than the equilibrium potential of the oxygen evolution reaction on the material surface, or in conditions where transpassivation is possible, the measured current density is subject to the influence of anodic currents from oxygen evolution and cannot be characterized as the beginning of pitting corrosion (E_{pit}). Depending on the environment, lower values of transpassive potentials have been reported for nickel alloys than for stainless steels increasing the influence of transpassivation on E_b for nickel-based alloys. This should also be taken into consideration for potentiostatic determinations of CPT, since the applied potential should not lead to transpassive corrosion of the tested material[13].

Nickel has been reported to have higher passive current densities than chromium-alloyed stainless steels. Considering this as true for high-nickel alloys, this could become a problem while attempting to set a critical current density for the propagation of local corrosion on these materials[14,15].

*e-mail: ivy_frazao@hotmail.com

The literature comparing pitting corrosion between nickel alloys and stainless steels through polarization tests is not properly discussed, since on authors knowledge there are not many studies in this area. Therefore this study aims to discuss both material classes regarding pitting corrosion using potentiostatic technique to determine the alloy's CPT values.

2. Experimental Procedures

Studied materials were provided as tubular products of UNS S32205, UNS S32750, UNS S32707, UNS N10276, UNS S31266 and UNS N06625 alloys, and were supplied by Sandvik Materials Technology. Table 1 summarizes the chemical composition and PRE of the materials.

Samples upon delivery conditions were cut and pressed in hot cured thermoset resin to obtain specimens where the working section corresponds to the tube cross section, with an exposed area of approximately 0.5 cm^2, with a surface finish provided by 600-grit silicon carbide abrasive paper. This was the sample preparation for the electrochemical tests. For microstructural characterization, similar specimens, polished up to a 1µm diamond finish were used to analyze the level of inclusions. The samples were submitted to electrolytic etching with 10% oxalic acid solution for 30 to 60 s at 6 Vcc and observed under optical microscope for microstructural characterization.

For the potentiostatic tests the electrolyte used is the 3M magnesium chloride ($MgCl_2$) solution with pH maintained between 6.5 and 7. An Autolab 20 potentiostat, controlled by NOVA 2.0 software, was used to control the applied potential, and current density recording.

A double wall electrochemical cell was used, with water flow as the heating media, up to 85° C. In the electrochemical cell, the counter electrode is a spiral wound platinum wire with an area at least 10 times larger than the working electrode, where the reference electrode was silver/silver chloride (Ag/AgCl) with 3,5M KCl.

For each material, potentiostatic polarization tests at 800 $mV_{Ag/AgCl}$ were performed by varying the temperature at a rate of 1°C/min, beginning polarization at 23°C and 5 minutes after immersion to ensure the same condition of the passive film and to allow stabilization of the initial temperature. During potentiostatic test the variation of current density as a function of temperature was recorded, and CPT was obtained when the current density reached a minimum of 100 µA/cm^2 and remained above this value for at least 60 s.

After electrochemical tests, the surface of the working electrodes was examined by optical microscopy to ensure that there was no crevice corrosion at the edges of the working electrode, which would invalidate the obtained CPT results.

3. Results and Discussion

Inclusion analyses revealed that the materials have type 1 fine series oxides inclusions, following the inclusion classification standards proposed by Jernkontoret[16]. The inclusions were found in small quantity and size for all materials, therefore they probably have small influence on the comparison of the obtained corrosion results for the alloys.

After etching the duplex alloys, metallographic examination indicated a ferritic microstructure matrix with austenite islands (Figure 1) which is expected for this class of materials, according to Naghizadeh and Moayed[17]. For UNS S31266 the micrography obtained (Figure 2) revealed the austenitic microstructure of the material without precipitation of intermetallic phases, as presented by Le Manchet and

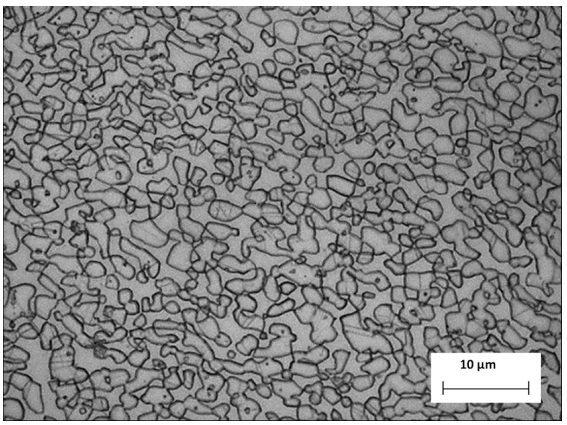

Figure 1. Cross section micrograph of the UNS S32205 sample after etching.

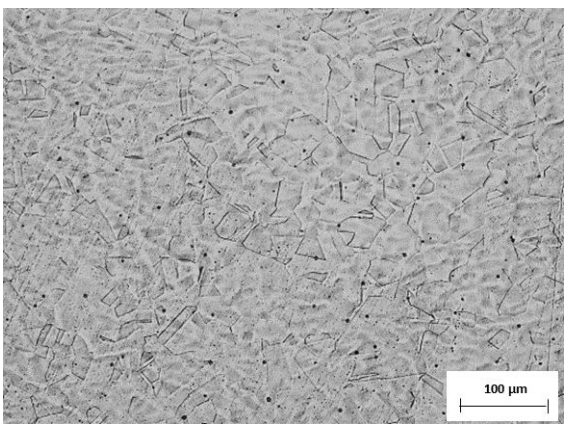

Figure 2. Cross section micrograph of the UNS S31266 sample after etching.

Table 1. Summary of the chemical composition of the materials studied (% by mass) and PRE.

UNS	%Cr	%Ni	%Mo	%N	%W	% Fe	PRE
S32205	22.2	5.23	3.14	0.17	-	balance	35.4
S32750	25.4	6.47	3.82	0.30	-	balance	42.8
S32707	26.7	6.37	4.77	0.38	-	balance	48.5
S31266	24.0	22.85	5.38	0.43	1.85	balance	48.7
N06625	21.4	balance	8.72	-		-	50.2
N10276	15.6	balance	15.5	-	3.73	-	66.8

Mottu-Bellier[18]. For the nickel-based alloys the microstructures obtained were also austenitic and a typical example is shown on (Figure 3), similar to the ones in literature[19].

All valid CPT results obtained through potentiostatic polarization are shown in Figure 4, where the materials are presented in ascending order of PRE. The results obtained between samples of the same material have low variation, showing that the proposed method generates accurate results and can be trusted within few tests. An exception is made for the results obtained for nickel-based alloys, since it was not possible to measure the CPT of UNS N10276 due to temperature limitation and frequent occurrence of crevice corrosion.

The potentiostatic polarization curves obtained for the studied alloys, including the nickel-based ones, can be seen in more details in Figures 5 to 10. The samples that presented crevice corrosion are available in dotted lines and those results were not considered valid.

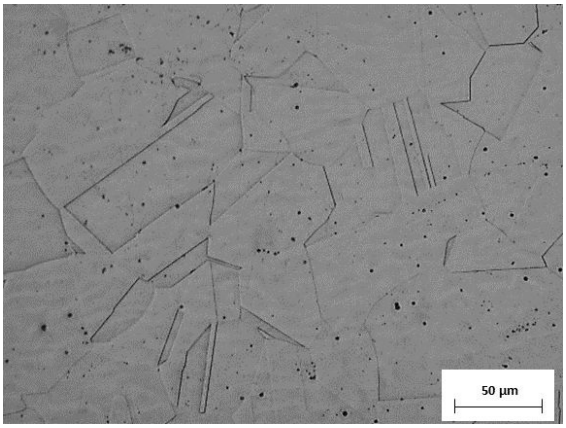

Figure 3. Cross section micrograph of the UNS N10276 sample after etching.

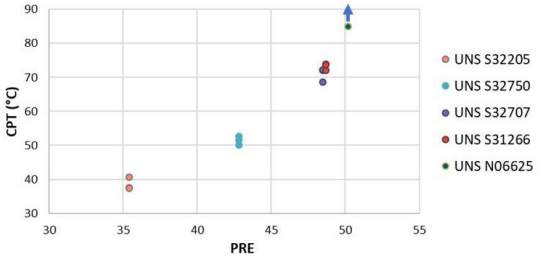

Figure 4. CPT results for the tested alloys.

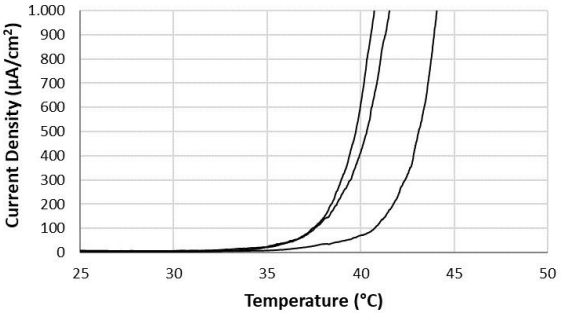

Figure 5. CPTs obtained for UNS S32205 samples.

It is also worth mentioning that it was possible to determine the CPT of UNS S32707 (Figure 7) and UNS N31266 (Figure 8) through the proposed method, which is a difficult task when 1M NaCl solution defined by ASTM G150[2] was used, since these materials have PRE greater

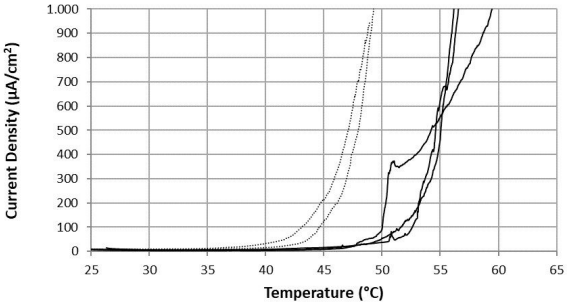

Figure 6. CPTs results of UNS S32750 samples. Crevice corrosion occurrence represented in dotted lines.

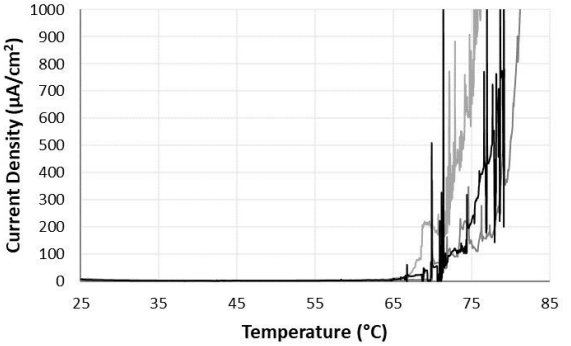

Figure 7. CPTs obtained for UNS S32707 samples.

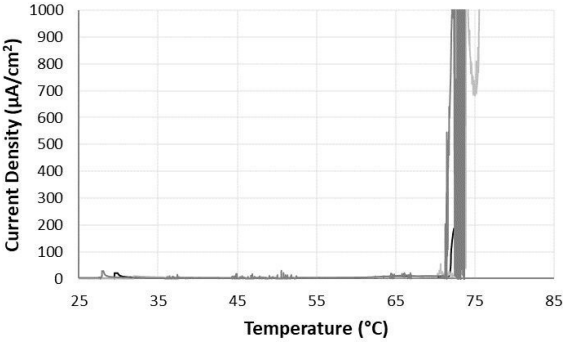

Figure 8. CPTs obtained for UNS S31266 samples.

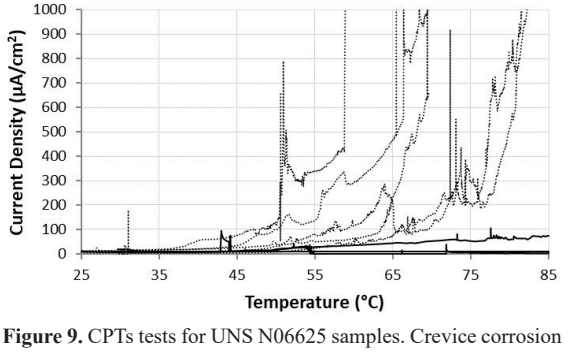

Figure 9. CPTs tests for UNS N06625 samples. Crevice corrosion occurrence represented in dotted lines.

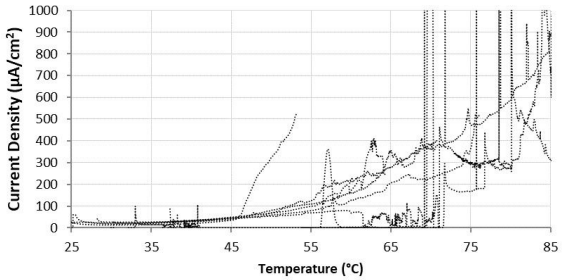

Figure 10. CPT tests for UNS N10276 samples. Crevice corrosion occurrence in all tests, represented in dotted lines.

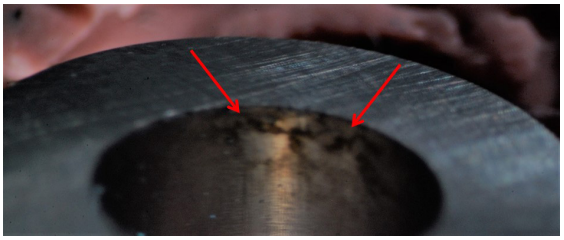

Figure 11. Crevice corrosion regions observed after CPT test for UNS N06625 sample, detached from the thermosetting resin.

than 47 and were expected to have CPT greater than 100°C in 1M NaCl[3].

For the nickel-based alloys, it was possible to determine the CPT of UNS N06625 as greater than 85°C (Figure 9), the maximum temperature used in the test. Precise value was not possible to be determined due to the temperature limitation of the heating fluid used. This CPT value is similar to results from Klapper, Zadorozne and Rebak[20] and Le Manchet and Mottu-Bellier[18] for immersion tests following ASTM G48[1]. Typical CPT-values of 75°C to 100°C were also identified after ASTM G48[1] tests according to VDM[21].

A high occurrence of crevice corrosion was observed for nickel-based alloys, making it impossible to determine CPT for the UNS N10276, and difficult to determine a precise CPT for UNS N06625, as previously mentioned. As shown in Figure 9 and Figure 10, the number of CPT tests performed for nickel-based alloys was greater than the number of tests required to determine the CPT of the stainless steels, showing a deficiency in the technique used to determine CPT for this class of materials. This deficiency was influenced by the apparatus used with tube samples cut and pressed in hot cured thermoset resin. Crevice corrosion regions were observed between the samples and the resin as exemplified in Figure 11.

The unexpected low crevice corrosion resistance found for nickel alloys has previously been reported by Delblanc et al.[22] and McCoy et al.[23]. Delblanc et al.[22] also observed that UNS N06625 has a high passive current compared to stainless steels, and while analyzing the chromium content on the crevice surface, they found chromium levels as low as 5 wt% for UNS N06625. For UNS N06625, the high current densities measured in potentiostatic test (Figure 9) at low temperatures could imply high passive currents. This could thus lead to a rapid IR-drop and then crevice solution quickly becomes more aggressive for UNS N06625. Shaw et al.[24] reported about IR drop (ohmic or potential drop of the creviced surface) for UNS N06625 and Betts and Boulton[25] demonstrated that migration of aggressive hydride and chloride ions into the crevice is enhanced with an increased IR-drop, corroborating this analysis.

Within the nickel based alloys studied there is a large difference between the CPT values and the critical crevice temperature (CCT). Considering ASTM G48[1] tests performed at UNS N10276[26], for example, the gap between CPT and CCT can reach 95°C, facilitating the appearance of crevice corrosion instead of pitting. For the studied stainless steels this gap is around 30°C[27].

4. Conclusions

The comparison between nickel alloys and stainless steels pitting corrosion through polarization tests still needs to be properly discussed and studied. With the results of this study it is possible to conclude:

- The method used for potentiostatic CPT measures was efficient to analyze stainless steels with high corrosion resistance but unable to determine accurately the CPT for nickel alloys due to temperature limitation, and test apparatus that lead to high tendency of crevice corrosion in nickel-based alloys.
- Nickel based alloys showed a higher susceptibility for crevice corrosion on CPT measurements when compared to stainless steel, which was not expected based on PRE analysis, indicating once more that these material class behave differently under corrosive environments.
- When comparing these material classes in a chloride containing environment the presence of crevices must be taken into consideration, as this study showed that the nickel base alloys can have a higher tendency for this corrosion type than the stainless steels.

5. References

1. American Society for Testing and Materials – ASTM. ASTM G48: pitting and crevice corrosion resistance of stainless steels and related alloys by use of ferric chloride solution. West Conshohocken: ASTM; 2015.
2. American Society for Testing and Materials – ASTM. ASTM G150: eletrochemical critical pitting temperature testing of stainless steels. West Conshohocken: ASTM; 2013.
3. Lund K, Delblanc A, Iversen A. Comparing critical pitting temperatures of stainless steels measured electrochemically in NaCl and $MgCl_2$ solutions. In: European Corrosion Congress (EUROCORR); 2016; Montpellier, France. Frankfurt am Main: DECHEMA e.V.; 2016.
4. Haugan EB, Næss M, Rodriguez CT, Johnsen R, Iannuzzi M. Effect of tungsten on the pitting and crevice corrosion resistance of type 25Cr super duplex stainless steel. Corrosion. 2017;73(1):53-67.
5. Sandvik. The role of duplex stainless steels in petrochemical heat exchanger applications. Sandviken: Sandvik Steel; 1997.
6. Spedo GRC. Avaliação de parâmetros de ensaio para determinação de temperatura crítica de pite em aço inoxidável dúplex por via potenciostática [dissertação]. São Bernardo do Campo: FEI University; 2018.
7. Werner H, Rommerskirchen I. Determination of critical pitting temperatures by calcium chloride test, results of round-robin test. Materials and Corrosion. 2007;58(10):767-73.
8. American Society for Testing and Materials – ASTM. ASTM G36: standard practice for evaluating stress corrosion cracking

resistance of metals and alloys in a boiling magnesium chloride solution. West Conshohocken: ASTM; 2013.
9. Arnvig P E, Bisgård AD. Determining the potential independent critical pitting temperature (CPT) by a potentiostatic method using the Avesta cell. In: Proceedings of Corrosion 96; 1996; Houston, TX. Houston: ACE Press; 1996. p. 437/1-437/17.
10. Kelly RG, Scully JR, Shoesmith D, Buchheit R. Electrochemical techniques in corrosion science and engineering. New York: Marcel Dekker; 2003.
11. Sedriks AJ. Corrosion of stainless steels. New York: Wiley, 1996.
12. Magnabosco R, Alonso-Falleiros N. Sigma phase formation and polarization response of UNSS31803 in sulfuric acid. Corrosion. 2005;61(8):807-14.
13. Qvarfort R, Olsson J. Transpassive corrosion of high alloy stainless steels and nickel-bases. In: Proceedings of Corrosion 2002; Denver. Denver, CO: NACE; 2002. (Paper no. 02133).
14. Flint GN, Oldfield JW. Nickel-iron alloys. In: Shreir LL, Jarman RA, Burstein GT, editors. Corrosion: metal/environment reactions. 3rd ed. Oxford: Butterworth-Heinemann; 1995. p. 3:92-3:100. (vol. 1).
15. Sato N. Basics of corrosion chemistry [Internet]. Berlin: Wiley-VCH Verlag GmbH & Co.; 2018 [cited 2018 Aug 21]. Available from: http://www.wiley-vch.de/books/sample/3527329307_c01.pdf
16. American Society for Testing and Materials – ASTM. ASTM E45: standard test methods for determining the inclusion content of steel. West Conshohocken: ASTM; 2007.
17. Naghizadeh M, Moayed MH. Investigation of the effect of solution annealing temperature on critical pitting temperature of 2205 duplex stainless steel by measuring pit solution chemistry. Corros Sci. 2015;94:179-89.
18. Le Manchet S, Mottu-Bellier N. Corrosion resistance of the super-austenitic material UNS S31266 in demanding environments. In: European Corrosion Congress (EUROCORR); 2016; Montpellier, France. Frankfurt am Main: DECHEMA e.V.; 2016. vol. 9, no. 52347.
19. American Society for Metals. ASM handbook: atlas of microstructure of industrial alloys. 8th ed. West Conshohocken: ASTM; ; 1972.
20. Klapper HS, Zadorozne NS, Rebak RB. Localized corrosion characteristics of nickel alloys: a review. Chin Shu Hsueh Pao. 2017;30:296-305.
21. VDM Metals. VDM® Alloy 625 Nicrofer 6020h, data sheet No. 4118, revision 03. Werdohl, Germany: VDM Metals International GmbH; 2018.
22. Delblanc A, Gullberg D, Mattsson R, Eidhagen J. Investigation of the crevice corrosion resistance of UNS S31266 and UNS N06625 using accelerated laboratory test methods. In: Proceedings of Corrosion 2019; 2019; Houston, TX. Houston: NACE; 2019. (Paper no. 13077).
23. McCoy SA, Puckett BC, Hibner EL. High performance age-hardenable nickel alloys solve problems in sour oil and gas service. Stainless Steel World. 2002;4:48-52.
24. Shaw BA, Moran PJ, Gartland PO. The role of ohmic potential drop in the initiation of crevice corrosion on alloy 625 in seawater. Corros Sci. 1991;32(7):707-19.
25. Betts AJ, Boulton LH. Crevice corrosion: review of mechanisms, modelling, and mitigation. Br Corros J. 1993;28(4):279-96.
26. Hastelloy. Hastelloy C-276 alloy [Internet]. 2020 [cited 2020 Feb 28]. Available from: http://haynesintl.com/docs/default-source/pdfs/new-alloy-brochures/corrosion-resistant-alloys/brochures
27. Sandvik. Sandvik SAF 2707: tube and pipe, seamless – datasheet [Internet]. 2020 [cited 2020 Feb 28]. Available from: https://www.materials.sandvik/en/materials-center/material-datasheets/tube-and-pipe-seamless